

HEAVY QUARK PAIR CORRELATIONS IN QCD

Yu.M.Shabelski and A.G.Shuvaev

Petersburg Nuclear Physics Institute,
Gatchina, St.Petersburg 188350 Russia

Abstract

The azimuthal correlations of heavy quarks produced in the high energy pp ($p\bar{p}$) collisions are calculated in the framework of QCD without the usual assumptions of the parton model. The virtual nature of the interacting gluons as well as their transverse motion and different polarizations are taken into account. We give some predictions for the azimuthal correlations of charm and beauty hadrons produced at Tevatron-collider and LHC.

E-mail SHABEL@VXDESY.DESY.DE

E-mail SHUVAEV@THD.PNPI.SPB.RU

1 INTRODUCTION

The investigation of the heavy quarks production in the high energy hadron processes provides a method for studying the internal structure of hadrons. Realistic estimates of the cross section of the heavy quark production as well as their correlations are necessary in order to plan experiments on existing and future accelerators. These predictions are obtained usually in the parton model framework and depend significantly on the quark and gluon structure functions. The last ones are more or less known experimentally from the data of HERA, but unknown at the very small values of Bjorken variable $x < 10^{-4}$. However it is just the region that dominates in the heavy quark production at the high energies.

The Gribov-Lipatov-Dokshitzer-Altarelli-Parisi (GLDAP) evolution equation is applied usually to calculate the structure functions. It sums up in the leading logarithm approximation (LLA) all the QCD diagram contributions proportional to $(\alpha_s \ln q^2)^n$, but it does not take into account the terms proportional to $(\alpha_s \ln 1/x)^n$. That is why this approximation does not give the correct asymptotic behaviour of the structure function in the small x region. For the correct description of these phenomena not only the terms of the form $(\alpha_s \ln q^2)^n$ have to be collected in the Feynman diagrams but also the terms $(\alpha_s \ln 1/x)^n$.

Another problem that appears at $x \sim 0$ is that of the absorption (screening) corrections which must stop the increase of the cross section at $x \rightarrow 0$ in accordance with the unitarity condition. It can be interpreted as the saturation of parton density. For relatively small virtuality $q^2 \leq q_0^2(x)$ the gluon structure function behaves as $xG(x, q^2) \sim q^2 R^2$, so the cross section for the interaction of the point-like parton with a target, $\sigma \sim (1/q^2)xG(x, q^2) \sim R^2$, obeys the unitarity condition. The quantity $q_0^2(x)$ can be treated as a new infrared-cutoff parameter which plays the role of the typical transverse momentum of partons in the parton cascade of the hadron in semihard processes. The behaviour of $q_0(x)$ was discussed in ref.[6]. It increases with $\log(1/x)$ and the values of $q_0(x)$ are about 2-4 GeV at $x = 0.01 - 0.001$.

The predictions for the cross section of the heavy quark pair production are based usually on the parton model calculations [1, 2]. All particles are assumed in this model to be on mass shell with the longitudinal component of the momentum only (so called collinear approximation), and the cross section is averaged over two transverse polarizations of the gluons. The virtualities q^2 of the initial partons are taken into account only through their densities. The latter are calculated in LLA through GLDAP evolution equation. The probabilistic picture of noninteracting partons underlies this way of proceeding. In the region, where the transverse mass m_T of the produced heavy

quark is close to $q_0(x)$, the dependence of the amplitude of the subprocess $gg \rightarrow \overline{Q}Q$, dominating at the high energy, on the virtualities and polarizations of the gluons becomes important. The amplitudes of these subprocesses should be calculated more accurately than in the parton model. The matrix elements of the QCD subprocesses accounting for the virtualities and polarizations of the gluons are very complicated. We presented them in our previous paper [4] for the main and simplest subprocesses, $gg \rightarrow \overline{Q}Q$ ($\sim \alpha_s^2$) for hadroproduction and $\gamma g \rightarrow \overline{Q}Q$ ($\sim \alpha_s$) for photo- and electroproduction. The contributions of high-order subprocesses can be essential, but our aim is to discuss the qualitative difference between our results and the parton model predictions. This can be done on the level of the low-order diagrams.

In this paper we calculate in the same order ($\sim \alpha_s^2$) the azimuthal correlations of the heavy quarks produced in hadron-hadron collisions which are in serious disagreement with the conventional parton model predictions (see [5] and references therein).

2 CROSS SECTIONS OF HEAVY FLAVOR PRODUCTION IN QCD

The cross section of heavy quark hadroproduction is given schematically by the diagrams in Fig.1. The main contribution to the cross section at small x is known to come from the gluons. The lower and upper ladder blocks represent the two-dimensional gluon distributions $\varphi(x, q_1^2)$ and $\varphi(x, q_2^2)$, which are the functions of the longitudinal momentum fraction (x and y) of the initial hadron and the virtuality of the gluon. Their distribution over x and transverse momenta q_T in hadron is given in semihard theory [1] by the function $\varphi(x, q^2)$. It differs from the usual function $G(x, q^2)$:

$$xG(x, q^2) = \frac{1}{4\sqrt{2}\pi^3} \int_0^{q^2} \varphi(x, q_1^2) dq_1^2. \quad (1)$$

Such a definition of $\varphi(x, q^2)$ enables to treat correctly the effects arising from the gluon virtualities. The exact expression for this function can be obtained as a solution of the evolution equation which, contrary to the parton model case, is nonlinear due to interactions between the partons in the small x region.

In what follows we use Sudakov decomposition for the quark momenta $p_{1,2}$ through the momenta of the colliding hadrons p_A and p_B ($p_A^2 = p_B^2 \simeq 0$) and the transverse ones $p_{1,2T}$:

$$p_{1,2} = x_{1,2}p_B + y_{1,2}p_A + p_{1,2T}. \quad (2)$$

The differential cross sections of heavy quarks hadroproduction have the form:¹

$$\begin{aligned} \frac{d\sigma_{pp}}{dy_1^* dy_2^* d^2p_{1T} d^2p_{2T}} &= \frac{1}{(2\pi)^8} \frac{1}{s^2} \int d^2q_{1T} d^2q_{2T} \delta(q_{1T} + q_{2T} - p_{1T} - p_{2T}) \\ &\times \frac{\alpha_s(q_1^2)}{q_1^2} \frac{\alpha_s(q_2^2)}{q_2^2} \varphi(q_1^2, y) \varphi(q_2^2, x) |M_{QQ}|^2. \end{aligned} \quad (3)$$

Here $s = 2p_A p_B$, $q_{1,2T}$ are the gluon transverse momenta and $y_{1,2}^*$ are the quark rapidities in the hadron-hadron c.m.s. frame,

$$\begin{aligned} x_1 &= \frac{m_{1T}}{\sqrt{s}} e^{-y_1^*}, & x_2 &= \frac{m_{2T}}{\sqrt{s}} e^{-y_2^*}, & x &= x_1 + x_2 \\ y_1 &= \frac{m_{1T}}{\sqrt{s}} e^{y_1^*}, & y_2 &= \frac{m_{2T}}{\sqrt{s}} e^{y_2^*}, & y &= y_1 + y_2. \end{aligned} \quad (4)$$

$|M_{QQ}|^2$ is the square of the matrix element for the heavy quark pair hadroproduction.

In LLA kinematics

$$q_1 \simeq yp_A + q_{1T}, \quad q_2 \simeq xp_B + q_{2T}, \quad (5)$$

so

$$q_1^2 \simeq -q_{1T}^2, \quad q_2^2 \simeq -q_{2T}^2. \quad (6)$$

(The more accurate relations are $q_1^2 = -\frac{q_{1T}^2}{1-y}$, $q_2^2 = -\frac{q_{2T}^2}{1-x}$, but we are working in the kinematics, where $x, y \sim 0$).

The matrix element M_{QQ} is calculated in the Born order of QCD without standart simplifications of the parton model, since in the small x domain there are no grounds for neglecting the transverse momenta of the gluons q_{1T} and q_{2T} in comparison with the quark mass and the parameter $q_0(x)$. In the axial gauge $p_B^\mu A_\mu = 0$ the gluon propagator takes the form $D_{\mu\nu}(q) = d_{\mu\nu}(q)/q^2$,

$$d_{\mu\nu}(q) = \delta_{\mu\nu} - (q^\mu p_B^\nu + q^\nu p_B^\mu)/(p_B q). \quad (7)$$

For the gluons in t -channel the main contribution comes from the so called 'nonsense' polarization $g_{\mu\nu}^n$, which can be picked out by decomposing the numerator into the longitudinal and the transverse parts:

$$\delta_{\mu\nu}(q) = 2(p_B^\mu p_A^\nu + p_A^\mu p_B^\nu)/s + \delta_{\mu\nu}^T \approx 2p_B^\mu p_A^\nu/s \equiv g_{\mu\nu}^n. \quad (8)$$

The other contributions are suppressed by the powers of s . Since the sum of the diagrams in Fig.1a-1c is gauge invariant in the LLA, the transversality

¹We put the argument of α_s to be equal to the gluon virtuality, which is very close to the BLM scheme[6]; (see also [7]).

condition for the ends of gluon line enables one to replace p_A^μ by $-q_{1T}^\mu/x$ in the expression for $g_{\mu\nu}^n$. Thus we get

$$d_{\mu\nu}(q) \approx -2 \frac{p_B^\mu q_T^\nu}{x s}, \quad (9)$$

or

$$d_{\mu\nu}(q) \approx 2 \frac{q_T^\mu q_T^\nu}{x y s}, \quad (10)$$

if we do such a trick for the vector p_B too. Both these equations for $d_{\mu\nu}$ can be used, but for the form (9) one has to modify slightly the gluon vertex (to account for the several ways of gluon emission — see ref. [8]):

$$\Gamma_{eff}^\nu = \frac{2}{x y s} [(x y s - q_{1T}^2) q_{1T}^\nu - q_{1T}^2 q_{2T}^\nu + 2x (q_{1T} q_{2T}) p_B^\nu]. \quad (11)$$

As a result the colliding gluons can be treated as aligned ones and their polarization vectors are directed along the transverse momenta. Ultimately, the nontrivial azimuthal correlations must arise between the transverse momenta p_{1T} and p_{2T} of the heavy quarks.

Formally, one loses the gauge invariance dealing with off mass shell gluons (q_1, q_2). Indeed, the new graphs similar to the 'bremsstrahlung' from the initial (final) quark line (Fig.1d) may contribute to the central plateau rapidity region in the covariant Feynman gauge. However this is not the fact. The function $\phi(x, q^2)$ collects with the "semihard" accuracy all terms of the form $\alpha_s^k (\ln q^2)^n (\ln(1/x))^m$ with $n + m \geq k$. In this case the triple gluon vertex (11) includes effectively all the main (leading logarithmic) contributions of the type of Fig.1d [9]. For example, the upper part of the graph shown in Fig.1d corresponds in terms of the BFKL equation to the t-channel gluon reggeization. Therefore the final expression is gauge invariant with the logarithmic accuracy.

Although the situation considered here seems to be quite opposite to the parton model, there is a certain limit in which our formulae can be transformed into the parton model ones. Consider the pp case and assume that the characteristic values of quark momenta p_{1T} and p_{2T} are much larger than the values of gluon momenta, q_{1T}, q_{2T} ,

$$\langle p_{1T} \rangle \gg \langle q_{1T} \rangle, \quad \langle p_{2T} \rangle \gg \langle q_{2T} \rangle, \quad (12)$$

and one can keep only the lowest powers of q_{1T}, q_{2T} . It means that we can put $q_{1T} = q_{2T} = 0$ everywhere in the matrix element M_{QQ} except the vertices. Introducing the polar coordinates

$$d^2 q_{1T} = \frac{1}{2} dq_{1T}^2 d\theta_1 \quad (13)$$

(and the same for q_{2T}) and performing angular integration with the help of the formula

$$\int_0^{2\pi} d\theta_1 q_{1T}^\mu q_{1T}^\nu = \pi q_{1T}^2 \delta_T^{\mu\nu} \quad (14)$$

we obtain

$$\int_0^{2\pi} d\theta_1 \frac{q_{1T}^\mu}{y} \frac{q_{1T}^\nu}{y} \int_0^{2\pi} d\theta_2 \frac{q_{2T}^\lambda}{x} \frac{q_{2T}^\sigma}{x} M_{\mu\nu} \overline{M}_{\lambda\sigma} = 2\pi^2 \frac{q_{1T}^2 q_{2T}^2}{(xy)^2} |M_{part}|^2. \quad (15)$$

Here M_{part} is just the parton model matrix element, since the result is the same as that calculated for the real (mass shell) gluons and averaged over transverse polarizations. Then we obtain the cross section (3) in the form [2, 3]:

$$\begin{aligned} & \frac{d\sigma}{dy_1^* dy_2^* d^2 p_{1T}} = \\ & = |M_{part}|^2 \frac{1}{(\hat{s})^2} \int \frac{\alpha_s(q_1^2) \varphi(y, q_{1T}^2)}{4\sqrt{2}\pi^3} \frac{\alpha_s(q_2^2) \varphi(x, q_{2T}^2)}{4\sqrt{2}\pi^3} dq_{1T}^2 dq_{2T}^2 = \\ & = \frac{\alpha_s^2(q^2)}{(\hat{s})^2} |M_{part}|^2 xG(x, q_2^2) yG(y, q_1^2), \end{aligned} \quad (16)$$

where $\hat{s} = xys$ is the mass square of $\overline{Q}Q$ pair.

On the other hand, the assumption (12) is not fulfilled in a more or less realistic case. The transverse momenta of produced quarks as well as the gluon virtualities (QCD scale values) should be of the order of heavy quark masses.

3 RESULTS OF CALCULATIONS

Eq.(3) enables to calculate straightforwardly the distributions over the azimuthal angle ϕ , which is defined as the opening angle between the two produced heavy quarks projected onto a plane perpendicular to the beam. Let us define this plane as xy -plane and let the first heavy quark flights to the x direction, i.e. $p_{1Tx} = p_{1T}$, $p_{1Ty} = 0$. In this case $\cos \phi = p_{2Tx}/p_{2T}$, and it is not a problem to evaluate the distribution over ϕ integrating Eq.(3) using, say, VEGAS code.

Since the functions $\varphi(x, q_2^2)$ and $\varphi(y, q_1^2)$ are unknown at the small values of q_2^2 and q_1^2 , we rewrite the integrals in Eq.(3) as

$$\int_0^\infty dq_{iT}^2 \delta(q_{iT} - p_{1T} - p_{2T}) \delta(y_1 + y_2 - 1) \frac{\alpha_s(q_i^2)}{q_i^2} \varphi(q_i^2, x) |M|^2 \frac{1}{y_2} =$$

$$\begin{aligned}
&= 4\sqrt{2}\pi^3\delta(p_{1T} + p_{2T})\delta(y_1 + y_2 - 1)\alpha_s(Q_0^2)xG(x, Q_0^2)\frac{1}{y_2}\left(\frac{|M|^2}{q_i^2}\right)_{q_i \rightarrow 0} \quad (17) \\
&\quad + \int_{Q_0^2}^{\infty} dq_{iT}^2\delta(q_{iT} - p_{1T} - p_{2T})\delta(y_1 + y_2 - 1)\frac{\alpha_s(q_i^2)}{q_i^2}\varphi(q_i^2, x)|M|^2\frac{1}{y_2},
\end{aligned}$$

where Eq.(1) is used². Thus, we obtain the sum of the three different contributions: the product of two first terms with $i = 1, 2$ in the r.h.s. of Eq.(17), $w_1(\phi)$; the sum of the products of first and second terms, $w_2(\phi)$; and, finally, the product of second terms, $w_3(\phi)$. The first contribution, $w_1(\phi)$, is very similar to the conventional LO parton model expression, in which the total heavy quark momenta is exactly zero and the angle between quarks is always 180° . However the angle between two heavy hadrons can be slightly different from this value due to a hadronization process. To take it into account we assume that in the first contribution, where quarks are produced back-to-back, the probability to find the final azimuthal angle ϕ ,

$$\sin\phi = \frac{p_h}{\sqrt{p_h^2 + p_T^2}}, \quad (18)$$

is determined by the expression

$$w(p_h) = \frac{2}{\sqrt{\pi}p_0}e^{-p_h^2/p_0^2}, \quad (19)$$

where $p_0 = 0.2$ GeV/c and p_h is the transverse momentum in the azimuthal plane of the hadron coming from hadronization process. The two last contributions, $w_2(\phi)$ and $w_3(\phi)$, result in a more or less broad distribution over the angle between the produced quarks, so we neglect here their small modification in the hadronization.

It is necessary to repeat that our approach is justified only at small x , that is at the high enough initial energies. Unfortunately, the highest energy, where the experimental data on the charm azimuthal correlations exist, is only $\sqrt{s} = 39$ GeV [5]. The values of q_1^2 and q_2^2 in Eq.(3), giving an essential contributions to the charm production cross section, are not large enough at this energy, so the first contribution in Eq.(17) dominates at the not very small Q_0^2 value and our predictions coincide practically with the results of LO parton model.

At the higher energies the second and third contributions become large enough and lead to some difference with the conventional parton model. The predictions of charm pair azimuthal correlations at $\sqrt{s} = 1800$ GeV and $Q_0^2 =$

²Here the value Q_0^2 should not be mixed with the function $q_0^2(x)$ discussed in the Introduction.

4 GeV² are presented in Fig.2a. The solid histogram shows the results for all produced charm particles. However in this case some hadronization mechanism can contribute to the azimuthal correlations of the charmed hadrons with the small relative momenta. To decrease this possible contribution the dashed histogram presents the same results for the events, where both charmed hadrons have the transverse momenta $p_T > p_{Tmin}$, $p_{Tmin} = 4$ GeV/c.

The same results at the energy $\sqrt{s} = 14$ TeV are shown in Fig.2b. Note that the predicted azimuthal correlations have some energy dependence, they become more broad, when the initial energy increases, however this energy dependence is weak enough, especially at $p_{Tmin} = 0$. Our ϕ -distributions seem to be more broad than the results of parton model calculations.

The similar predictions for the beauty pair azimuthal correlations at the energies $\sqrt{s} = 1800$ GeV and 14 TeV are presented in Fig.3 for the two values of p_{Tmin} , 0 and 8 GeV/c. For both these p_{Tmin} values the distributions become more broad with the energy increase.

Contrary to the parton model results, we predict two peaks for all cases, the standard one at $\phi = 180^\circ$ and the second peak with the smaller altitude, at $\phi = 0^\circ$, originated from the contribution of the diagram Fig.1c.

The HERA experimental data on $F_2(x, Q^2)$ at the small x , actually $10^{-4} < x < 10^{-2}$, show the singular x -behaviour at the moderate Q^2 (say, $Q^2 \sim 10^1$ GeV²). Both ZEUS [11] as well as H1 [12] Coll. data can be parametrized as $x^{-\delta}$ with $\delta = 0.1 \div 0.25$. Such a behaviour at $x \rightarrow 0$ is in evident contradiction with the unitarity and has to be stopped by a shadow mechanism [1, 13, 14].

To see the possible influence of the shadow effects on the azimuthal correlations we make the simplest assumption that the shadowing modifies the gluon distribution in such a way that the real distribution can be written as

$$xG(x, Q^2) = \frac{xG_0(x, Q^2)}{1 + \epsilon xG_0(x, Q^2)}, \quad (20)$$

where $\epsilon \ll 1$ and $xG_0(x, Q^2)$ is the bare GRV (HO) gluon distribution [10]. Both $xG(x, Q^2)$ and $xG_0(x, Q^2)$ distributions are shown in Fig.4 for the value $\epsilon = 0.01$. One can see that the difference between them at the smallest x , where the data exist ($x \sim 10^{-4}$), is about 10 %.

The calculated results for the azimuthal correlations of the heavy flavour pairs with "shadowed" gluon distributions, Eq.(20), are presented in Fig.5 and show that the shadowing does not significantly affect our results.

4 CONCLUSION

The above discussion shows that the accounting for the virtual nature of the interacting gluons as well as their transverse motion and different polariza-

tions results in the qualitative discrepancies with the parton model predictions. Using, say, LO QCD formulae we obtain a considerably more broad distribution over the angle between two heavy flavours than the convenient NLO parton model (see [5]). The reason is that the NLO parton model allows the discussed distributions to differ from δ -functions only due to the emission of one hard gluon. Our approach, to the contrary, incorporates effectively the emission of all evolution gluons via the phenomenological gluon distribution.

We are grateful to M.G.Ryskin for useful discussions and to E.M.Levin who participated at the early stage of the calculations.

This work is supported in part by INTAS-93-0079, Russian Fund of Fundamental Research (95-2-03145) and the Volkswagen Stiftung.

Figure captions

Fig. 1. Low order QCD diagrams for the heavy quark production in pp ($p\bar{p}$) collisions via gluon-gluon fusion (a-c) and the diagram (d) violating formally the gauge invariance, which is restored, however, with logarithmic accuracy.

Fig. 2. The calculated azimuthal correlations of the charm pair production in pp ($p\bar{p}$) collisions at $\sqrt{s} = 1800$ GeV (a) and $\sqrt{s} = 14$ TeV (b) for all events (solid histograms) and for the events, where both the charm particles have $p_T > p_{Tmin}$ (dashed histograms).

Fig. 3. The calculated azimuthal correlations of the beauty pair production in pp ($p\bar{p}$) collisions at $\sqrt{s} = 1800$ GeV (a) and 14 TeV (b) for all events (solid histograms) and for the events, where both the beauty particles have $p_T > p_{Tmin}$ (dashed histograms).

Fig. 4. Gluon structure function of the nucleon [10] without (solid curve) and with (dashed curve) shadow correction, Eq.(19).

Fig. 5. The calculated azimuthal correlations of charm (a) and beauty (b) pair production in pp ($p\bar{p}$) collisions at $\sqrt{s} = 14$ TeV for all events (solid histograms) and for the events, where both the heavy flavour particles have $p_T > p_{Tmin}$ (dashed histograms).

References

- [1] L.V.Gribov, E.M.Levin and M.G.Ryskin. Phys.Rep. 100 (1983) 1;
E.M.Levin and M.G.Ryskin. Phys.Rep. 189 (1990) 267.
- [2] P.Nason, S.Dawson and R.K.Ellis. Nucl.Phys. B303 (1988) 607.
- [3] G.Altarelli. Nucl.Phys. B308 (1988) 724.
- [4] M.G.Ryskin, Yu.M.Shabelski and A.G.Shuvaev. Z.Phys. C69 (1996) 269.
- [5] BEAT Coll., M.Adamovich et al. Phys. Lett. B348 (1995) 256.
- [6] S.J.Brodsky, G.P.Lepage and P.B.Mackenzie. Phys.Rev. D28 (1983) 228.
- [7] E.M.Levin, M.G.Ryskin, Yu.M.Shabelski and A.G.Shuvaev. Yad.Fiz. 54 (1991) 1420.
- [8] E.M.Levin, M.G.Ryskin, Yu.M.Shabelski and A.G.Shuvaev. Yad.Fiz. 53 (1991) 1059.
- [9] E.A.Kuraev, L.N.Lipatov, V.S.Fadin: Sov. Phys. JETP 45 (1977) 199.
- [10] Gluck, Reya and A.Vogt. Z.Phys. B263 (1991) 579.
- [11] ZEUS Coll., M.Derrick et al. Phys. Lett. B345 (1995) 576.
- [12] H1 Coll., S.Aid et al. Phys. Lett. B354 (1995) 494.
- [13] A.H.Mueller and J.Qiu. Nucl.Phys. B268, (1986) 427.
- [14] J.Kwiechinski, A.D.Martin, W.J.Stirling and R.G.Roberts. Phys.Rev. D42 (1990) 3645.

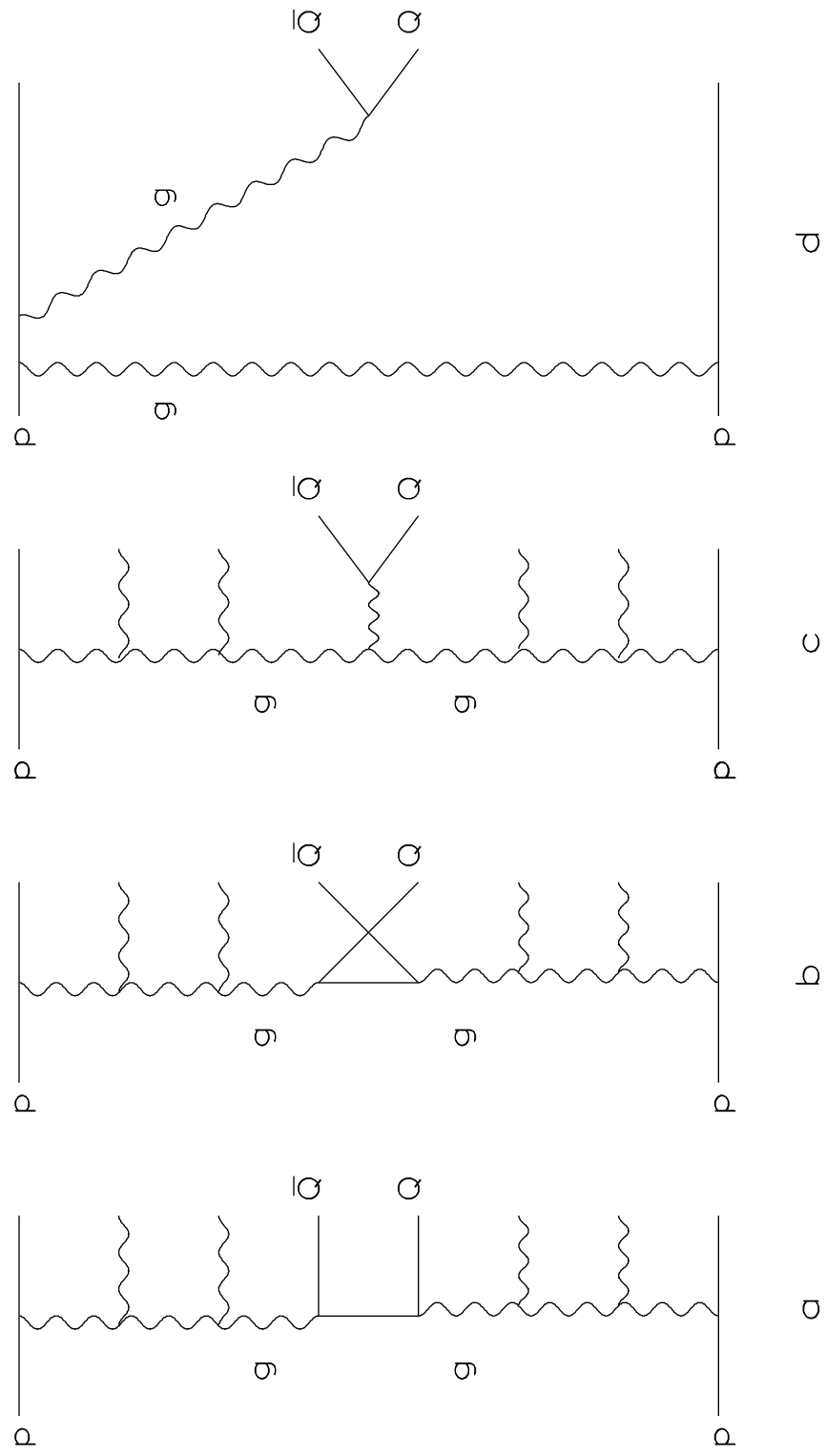


Fig. 1

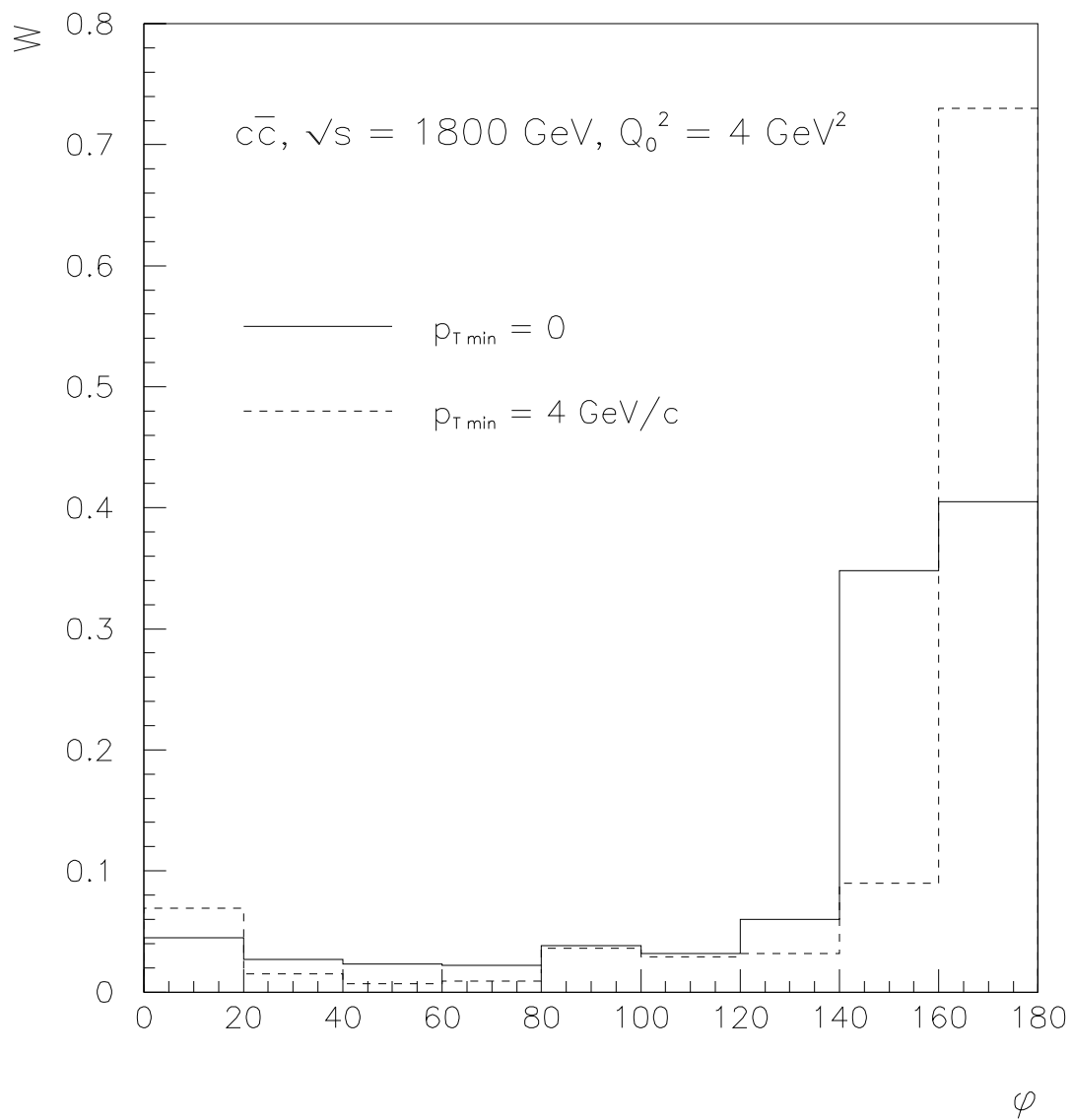


Fig. 2a

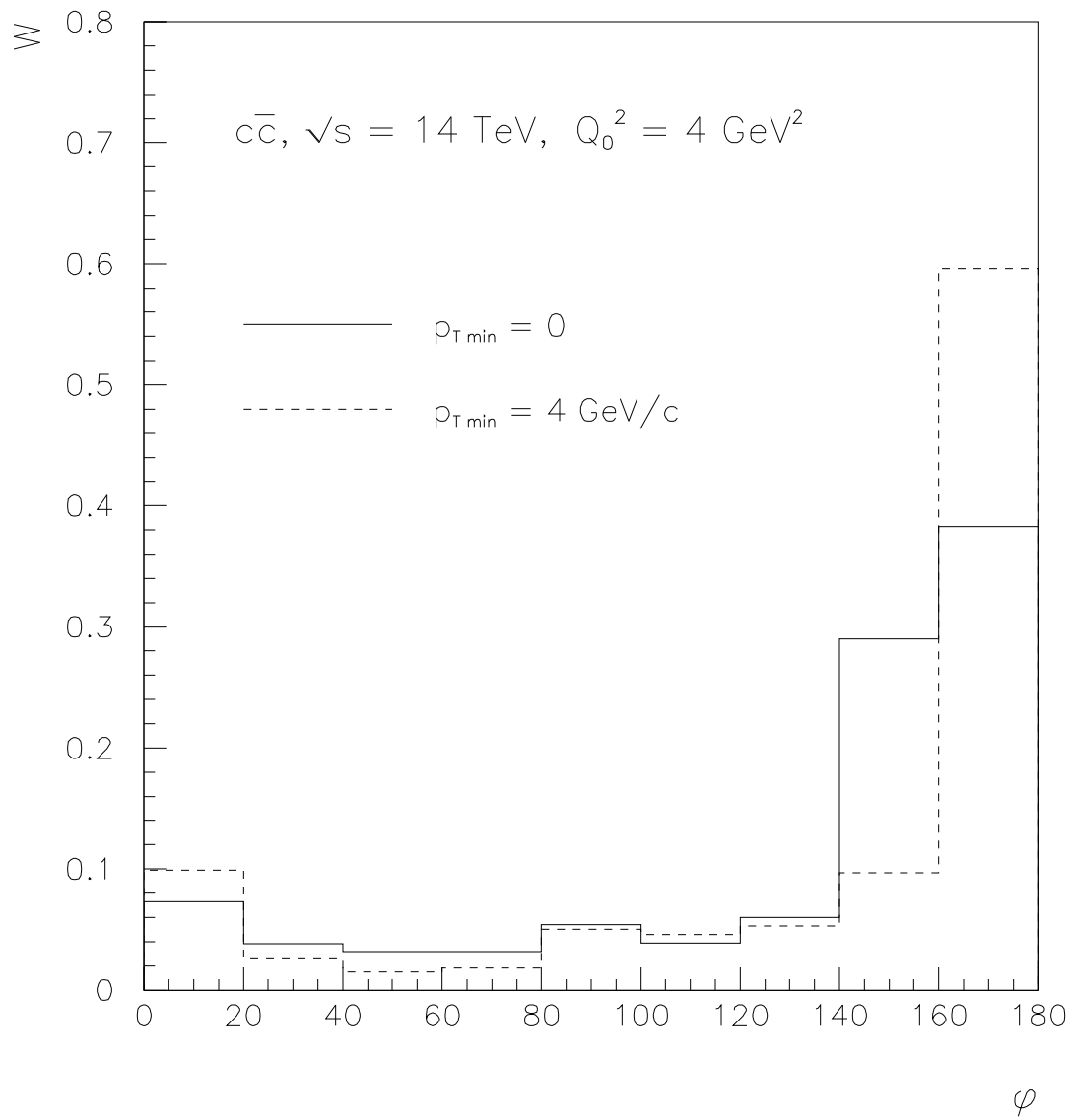


Fig. 2b

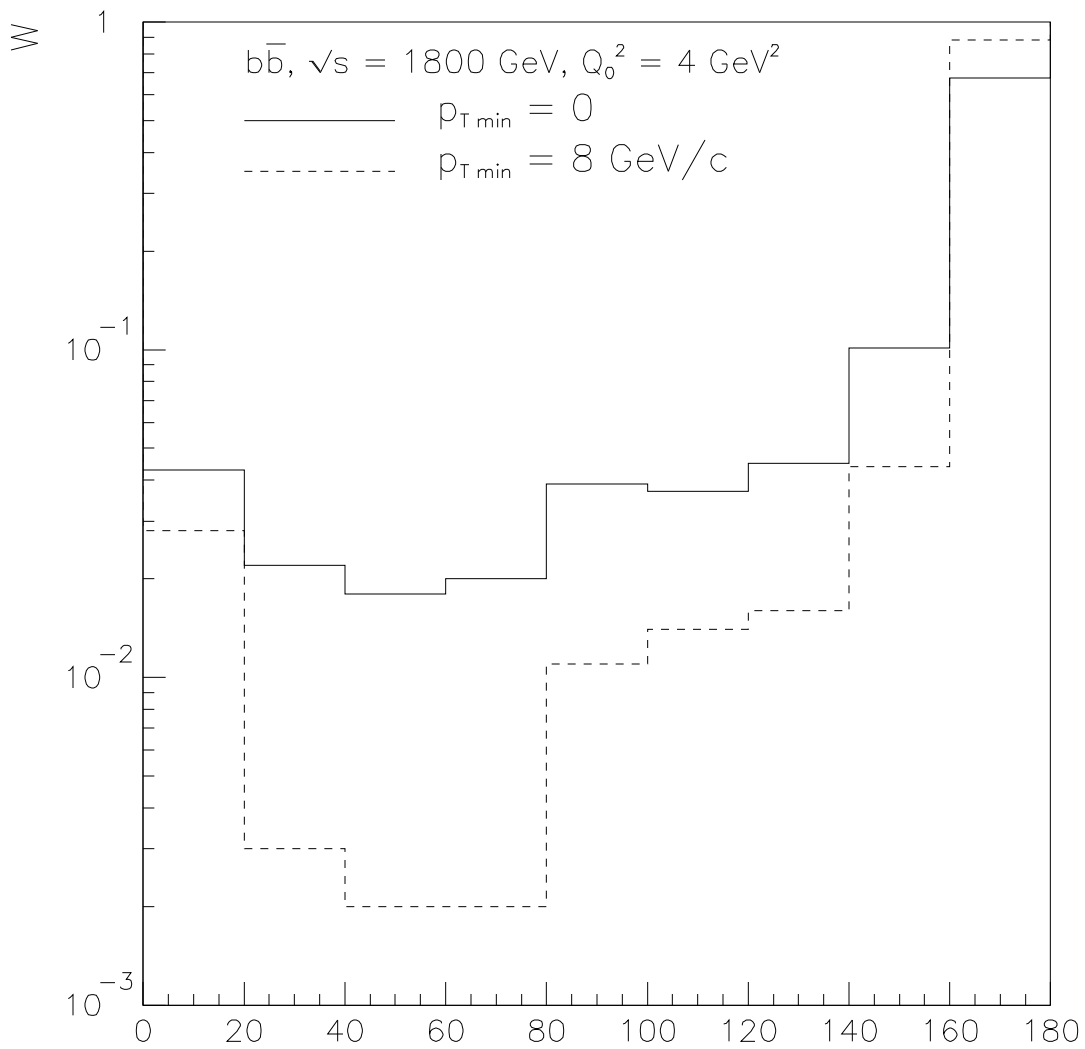


Fig. 3a

φ

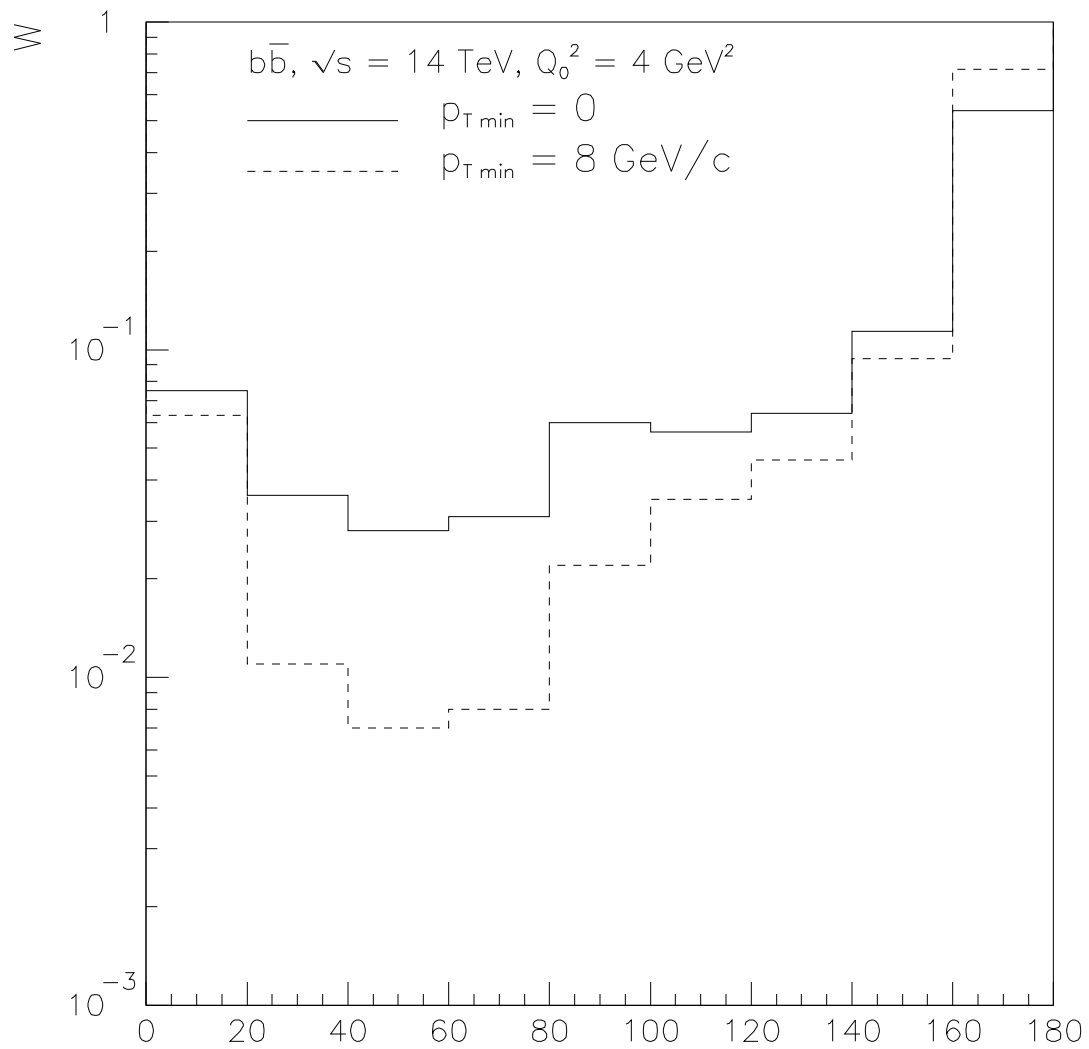


Fig. 3b

φ

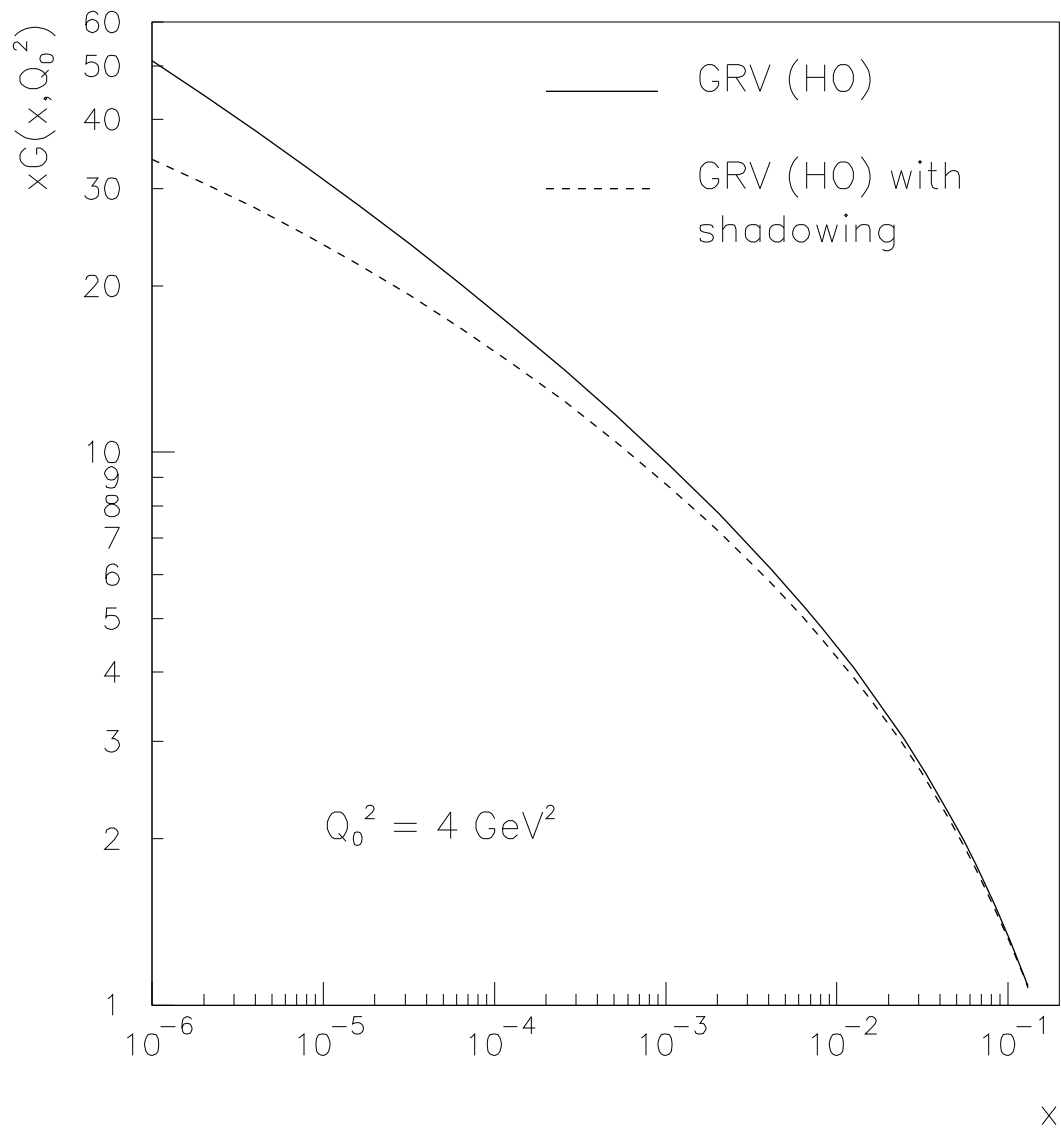


Fig. 4

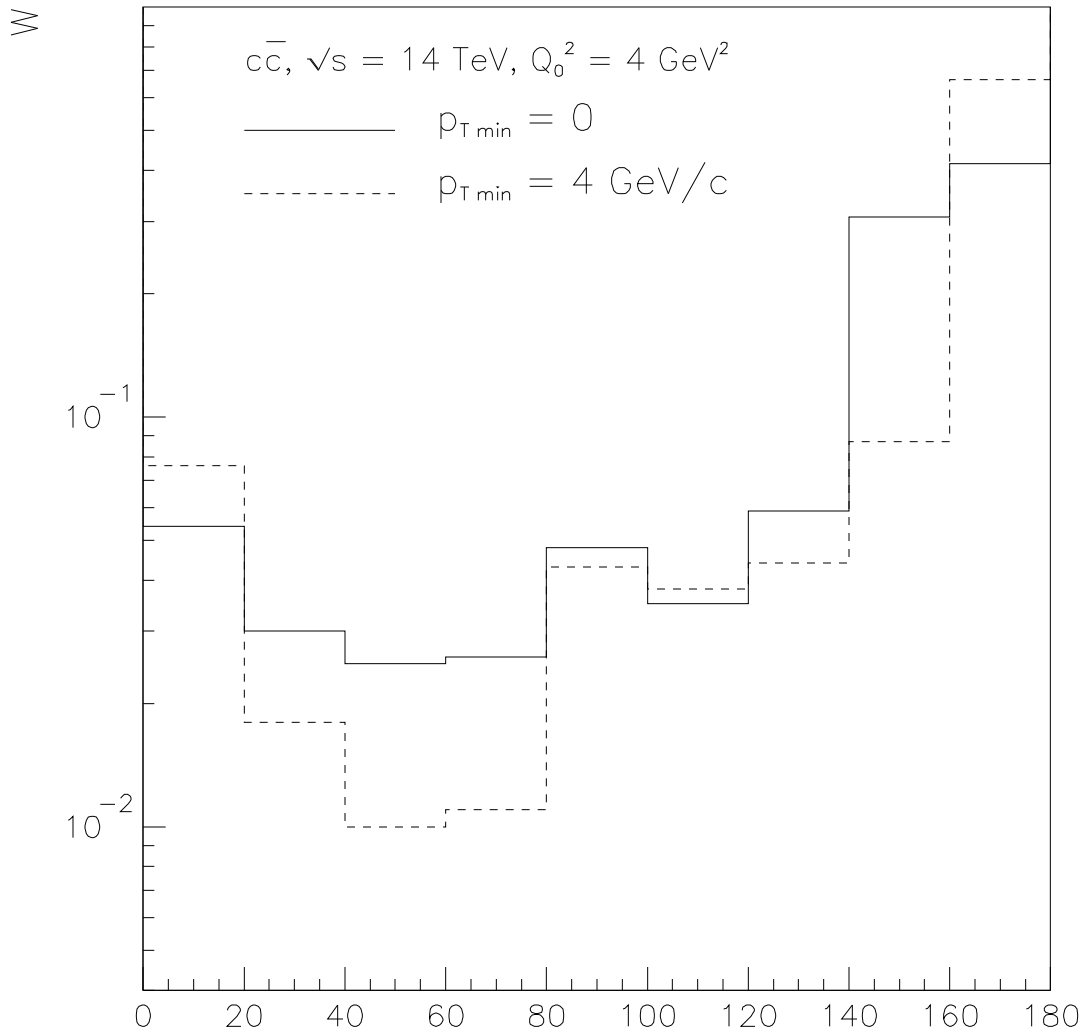


Fig. 5a

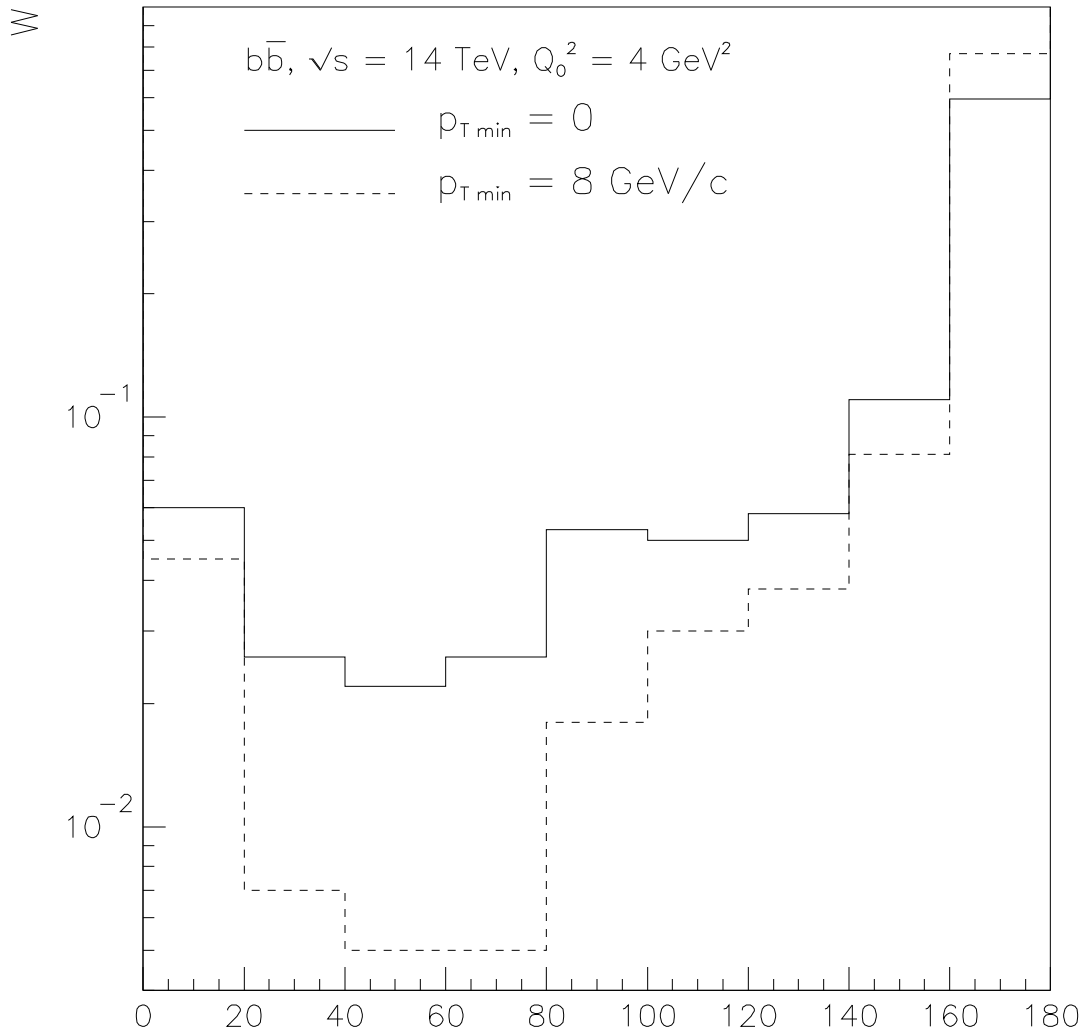


Fig. 5b